



ELSEVIER

1 February 1998

OPTICS  
COMMUNICATIONS

Optics Communications 147 (1998) 107–111

# Efficient room temperature LiF:F<sub>2</sub><sup>+</sup> color center laser tunable in 820–1210 nm range

Alex Yu. Dergachev<sup>1</sup>, Sergey B. Mirov*Department of Physics, University of Alabama at Birmingham, Birmingham, AL 35294, USA*

Received 31 July 1997; revised 21 October 1997; accepted 23 October 1997

## Abstract

Efficient room temperature operation of a LiF:F<sub>2</sub><sup>+</sup> color center laser at record levels of output energy (up to ~100 mJ) and average power (up to ~1.4 W) with a very wide 796–1210 nm tuning range is described. A photo- and thermostable lasing was realized due to: (i) improved technology of LiF crystals with stabilized F<sub>2</sub><sup>+</sup> color centers and (ii) appropriate choice of the pumping laser wavelength. Record real efficiencies for LiF:F<sub>2</sub><sup>+</sup> laser, 28% under pumping by radiation of an alexandrite laser (740 nm) and 53% under pumping by Raman shifted (H<sub>2</sub> and D<sub>2</sub>) second harmonic of a Nd:YAG laser (683 and 633 nm), were achieved. © 1998 Elsevier Science B.V.

PACS: 42.55.Qy; 42.60.Fc; 42.60.Jf; 78.50.Ec; 78.55.Hx

Keywords: Color center laser; Tunable laser; LiF:F<sub>2</sub><sup>+</sup>; Alexandrite laser

## 1. Introduction

LiF:F<sub>2</sub><sup>+</sup> is a high gain active medium with large absorption and emission cross-sections, and a wide near IR tuning range [1,2]. Unfortunately, low thermal stability of ‘‘pure’’ F<sub>2</sub><sup>+</sup> centers at room temperature (half decay time ~12 hours) made the LiF:F<sub>2</sub><sup>+</sup> laser medium very inconvenient for use, as it could be operated only at temperatures <100 K [1].

In 1978, Khulugurov and Lobanov [3] discovered that thermal stability of positively charged ‘‘pure’’ F<sub>2</sub><sup>+</sup> centers could be increased by co-doping LiF crystals with suitable anion or cation impurities, with formation of complex F<sub>2</sub><sup>+</sup>-like centers. However, the improved thermostability of these centers at room temperature did not provide appropriate photostability of active media under powerful laser excitation at wavelengths ≤590 nm. For example, pumping of LiF crystals with F<sub>2</sub><sup>+</sup>-stabilized color centers by

powerful radiation of the second harmonic of a Nd:YAG laser (532 nm) results in significant fading of the color center laser output [4], although, at low levels of pumping (several tens of millijoules), the color center laser will operate relatively well [5]. The fading under high power excitation is caused by the photo-chemical process in the pumping channel of the crystal, which involves two-step photoionization of neutral F<sub>2</sub> centers (F<sub>2</sub> + 2hν = F<sub>2</sub><sup>+</sup> + e) and trapping of the released electron e by the positively charged F<sub>2</sub><sup>+</sup> centers (F<sub>2</sub><sup>+</sup> + e = F<sub>2</sub><sup>•+</sup>). Concentration of ‘‘pure’’ F<sub>2</sub><sup>+</sup> centers which appeared due to photoionization of F<sub>2</sub> centers quickly reduces as F<sub>2</sub><sup>+</sup> centers migrate through the crystal with creation of F<sub>3</sub><sup>+</sup> centers: F<sub>2</sub><sup>+</sup> + F = F<sub>3</sub><sup>+</sup> [6].

In this paper, we report on the development of a high power room temperature photo- and thermostable tunable LiF:F<sub>2</sub><sup>+</sup> laser. The optimized technology of thermostable F<sub>2</sub><sup>+</sup> color center in LiF crystals and appropriate choice of the pumping laser wavelength allow for simultaneous solution of the problems of photo- and thermostability of laser materials based on LiF crystals with F<sub>2</sub><sup>+</sup>-like color centers.

<sup>1</sup> Present address: Schwartz Electro-Optics Inc., 135 South Rd., Bedford, MA 01730, USA.

## 2. Technological aspects of $\text{LiF:F}_2^{+*}$ crystal preparation

The peculiarities of technological preparation of  $\text{LiF:F}_2^{+*}$  crystals are given in our recent study [7]. The crystals were grown by the Kyropulos method, in argon atmosphere, from nominally pure raw materials, and doped with  $\text{LiOH}$ ,  $\text{Li}_2\text{O}$  and  $\text{MgF}_2$ . In order to obtain a high concentration of  $\text{F}_2^{+*}$  centers and a small concentration of colloids and parasitic aggregate color centers, grown crystals were subjected to a multi-step  $\gamma$ -irradiation treatment with a  $\text{Co}^{60}$  source [7].

The most important difference between the stabilized  $\text{LiF:F}_2^{+*}$  crystals described in the current paper and  $\text{LiF:F}_2^{+*}$ -like crystals reported in the literature [1–3.5] is the technology of multistage irradiation and thermal treatment of impurity doped LiF crystals. The proposed technology simultaneously provides efficient thermal stabilization of  $\text{F}_2^{+*}$  like centers, the highest possible concentration of these centers at a small level of optical losses, and significantly reduces the efficiency of formation of color centers – donors of electrons. The latter dramatically improves the overall photostability of the crystal under powerful laser excitation.

As grown LiF crystals have intense infrared absorption band at  $\nu_m = 3730 \text{ cm}^{-1}$  (absorption coefficient  $\sim 1.2 \text{ cm}^{-1}$ ) due to  $\text{OH}^-$  ions, which substitute fluoride in the anion node of the crystalline lattice, and intense bands with frequency maxima at  $3560$  and  $3610 \text{ cm}^{-1}$ , due to  $\text{Mg}^{2+}\text{OH}^-\text{OH}^-\text{V}_c^-$  complexes. UV absorption spectra of the grown LiF crystals exhibit strong absorption bands in the region  $200\text{--}270 \text{ nm}$  that are due to the  $\text{O}^{2-}\text{--V}_a^+$  as well as  $\text{O}^{2-}\text{--Mg}^{2+}$  dipoles.

The efficiency of formation of any type of color centers depends on the temperature of irradiation and storage of the crystal, impurity composition of the initial material, ionizing radiation dose power and irradiation dose. The optimized irradiation treatment to create  $\text{F}_2^{+*}$  stabilized color centers in doped LiF crystals is discussed below.

At the first stage the crystals are subjected to an ionizing treatment ( $\gamma$ -irradiation,  $(2\text{--}5) \times 10^7 \text{ R}$ ) at temperatures lower than the temperature  $T(\text{V}_a^+) = 240 \text{ K}$  of anion vacancy ( $\text{V}_a^+$ ) mobility in LiF crystals.

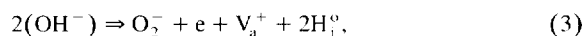
Ionizing treatment creates a great number of free electrons and holes, which can form self-localized excitons after thermalization. These excitons localized near a specific anion node of the crystalline lattice may annihilate and the released energy can be used for shifting an ion from its node to the interstitial position causing formation of an anion vacancy and an F center according to the schemes [8]:



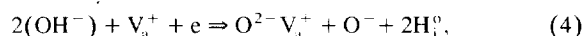
where F is an F-center and H is an interstitial halogen

atom. A fast recharging of F–H pairs under flux of electrons gives rise to actually simultaneous formation of the anion vacancies  $\text{V}_a^+$  and interstitial halogen ions  $\text{I}_a^-$  [9].

Simultaneously with primary defect formation according to (1) and (2), two processes of  $(\text{OH})^-$  ion dissociation are taking place under ionizing treatment [10]:



and



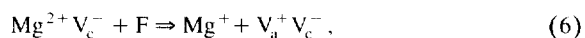
where  $\text{O}_2^-$  is a molecular ion of oxygen,  $\text{O}^-$  is a single ionized atom of oxygen, and  $\text{H}_i^0$  is an interstitial atom of hydrogen.

It is very important that there is no formation of aggregate color centers during irradiation of the crystal at temperatures below the temperature of mobility of anion vacancies.  $\text{O}^{2-}\text{--V}_a^+$  dipoles are accumulated in a high quantity, since they are photo- and thermostable under  $\gamma$ -irradiation. In addition to this, ionizing treatment creates a high concentration of single ionized oxygen atoms and molecules due to a hydroxyl group dissociation. It is noteworthy to mention that one of the products of  $\text{OH}^-$  radiolysis – interstitial  $\text{H}_i^0$  atoms are efficient traps of electrons:



which prevent the electrons from being captured by the  $\text{F}_2^{+*}$  center at the subsequent stages of crystal preparation, thereby increasing the efficiency of accumulation of stable  $\text{F}_2^{+*}$  centers.

The role of Mg impurity can be explained as follows. The F-center formation is likely to occur near the impurity-cation vacancy dipole  $\text{Mg}^{2+}\text{--V}_c^-$ . In accordance with the following reaction:



an F center can give its electron to a divalent metal impurity forming  $\text{Mg}^+$  and a pair of vacancies  $\text{V}_a^+\text{V}_c^-$ . Anion–cation dipoles  $\text{V}_a^+\text{V}_c^-$  play an important role in the formation of  $\text{F}_2^{+*}$  perturbed color centers at the subsequent stages of crystal preparation. However, excessive concentration of Mg dopant may play a negative role due to decreasing concentration of the useful  $\text{O}^{2-}\text{--V}_a^+$  dipoles by bonding with oxygen and formation of  $\text{Mg}^{2+}\text{O}^{2-}$  dipoles that do not take part in  $\text{F}_2^{+*}$  like center formation.

At the second stage of the technological process, the crystals are heated up to  $T_1 < T < T_2$ , where  $T_1$  ( $\sim 240 \text{ K}$ ) is the threshold temperature of  $\text{V}_a^+$  mobility and  $T_2$  ( $\sim 270 \text{ K}$ ) of  $\text{F}_2^{+*}$ ,  $\text{V}_a^+\text{V}_c^-$  and  $\text{O}^{2-}\text{--V}_a^+$  mobility in a LiF crystal, and stored at this temperature for some time. The above mentioned temperature interval is chosen within these specific limits so that anion vacancies are mobile in the crystal and  $\text{F}_2^{+*}$  centers as well as  $\text{V}_a^+\text{V}_c^-$  and  $\text{O}^{2-}\text{--V}_a^+$  dipoles are frozen and cannot diffuse in the crystalline

lattice. During this time an important process of formation of unperturbed  $F_2^+$  color centers takes place due to diffusion of mobile anion vacancies and their association with F centers:



Consequently the concentration of F centers is decreased due to their association with anion vacancies. It is a useful process helping to increase the concentration of  $F_2^+$  stabilized centers at the following stages and decrease the concentration of other aggregates and colloids.

At the third stage the crystals are re-irradiated at the temperature  $T < T_1$  in order to increase the amount of anion vacancies (that have been exhausted at the second stage) by ionizing the neutral F centers. After that the crystals are again subjected to the procedure described for stage two in order to increase the amount of pure  $F_2^+$  centers due to process (7).

At the fourth stage the crystals are heated up to room temperature and stored for some period of time, after which the crystals exhibit a stable concentration of the color centers of interest and are ready for use as a laser medium. The processes that take place at this stage are as follows.

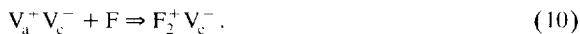
(i) The  $O^{2-}V_a^-$  complexes are mobile at room temperature and their migration leads to the development of  $F_2^{+*}$  centers stabilized with the  $O^{2-}$  ion ( $F_2^+O^{2-}$ ):



(ii) Another very important reaction occurs due to the intrinsic mobility of  $F_2^+$  centers at room temperature. The migration of these centers may lead to a useful process of association of  $F_2^+$  centers with a single ionized oxygen atom  $O^-$  with  $F_2^+O^{2-}$  center formation:



(iii) Since at room temperature bi-vacancy dipoles  $V_a^+V_c^-$  are also mobile ( $V_a^+V_c^-$  start to be mobile at a temperature of about 273 K) they may associate with F centers and perturbed  $F_2^+$  centers occur:



Due to the described LiF crystal multistage treatment, the optimum conditions for useful processes (8)–(10) of  $F_2^+$  stabilized color center formation are provided and the efficiency of the parasitic processes ( $F_2^+ + e \Rightarrow F_2$ ,  $F_2 + e \Rightarrow F_2^-$ ,  $F_2^+ + F \Rightarrow F_3^+$ ,  $F_2^+ + F_2 \Rightarrow F_4^+$ ,  $F_2^+ + F_2^- \Rightarrow F_4$ ,  $V_a^- + F_2 \Rightarrow F_3^+$ ) responsible for formation of other aggregates and colloid centers is suppressed.

### 3. Experimental results and discussion

Absorption and luminescence spectra of our LiF: $F_2^{+*}$  laser crystals, shown in Fig. 1 were corrected for the

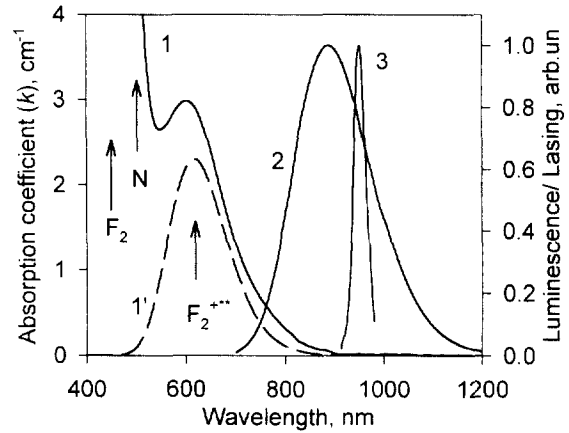


Fig. 1. Absorption (1), deconvoluted absorption (1'), luminescence (2) and lasing (3) spectra (in non-selective resonator) of  $F_2^{+*}$  color centers in LiF laser crystal at 300 K.

spectral response of the detection systems.  $F_2^{+*}$  color centers featured quasi-homogeneously broadened absorption ( $\lambda_{max} \sim 620$  nm,  $\Delta\nu \sim 3550$   $cm^{-1}$ ) and wide luminescence ( $\lambda_{max} \sim 890$  nm,  $\Delta\nu \sim 2300$   $cm^{-1}$ ) bands, short exponential luminescence decay with lifetime of 20 ns at 300 K and 37.5 ns at 77 K, high emission cross section ( $\sigma_e = 5.7 \times 10^{-17}$   $cm^2$  at 890 nm), and high quantum efficiency of luminescence  $\sim 55\%$  at 300 K. A high concentration of active  $F_2^{+*}$  centers ( $(4-8) \times 10^{16}$   $cm^{-3}$ ) at a low level of losses (contrast  $\sim 40$ ) was obtained.

As can be seen in Fig. 1, the absorption range (i.e. suitable pumping range) of  $F_2^{+*}$  laser crystals is between 500 and 800 nm. The threshold wavelength for  $F_2$  center two-step photoionization in LiF is about 590 nm [2]. Therefore in order to decrease absorption by  $F_2$  and N centers and avoid photoionization of  $F_2$  centers (Fig. 1, curve 1), it is necessary to shift the excitation to the long wavelength part of the  $F_2^{+*}$  absorption band (620–750 nm). That is why the wavelength range of an alexandrite laser, which emits in the 700–800 nm range, or the 1st Stokes component at 683 nm or 633 nm of a Raman shifted ( $H_2$  or  $D_2$ ) frequency doubled Nd:YAG laser makes them very attractive pumping sources for a LiF: $F_2^{+*}$  laser.

Initial experiments with a LiF: $F_2^{+*}$  laser were performed in a simple flat–flat resonator, set to a length of  $\sim 20$  cm. The active element, with Brewster faces, had 40 mm length and clear aperture of  $8 \times 8$  mm. The input dichroic mirror transmitted  $\geq 93\%$  at 633, 683 and 740 nm and reflected  $\geq 99\%$  in the 875–1040 nm range. The output coupler transmitted  $\sim 50\%$  in the 800–1100 nm range. An unfocused pumping beam from an alexandrite laser was introduced into a LiF crystal through the dichroic mirror. The optimum pumping wavelength was determined experimentally to be  $\sim 740$  nm. Because the alexandrite

laser has maximum output energy at  $\sim 750$  nm, with a sharp drop to 720 nm, the pumping wavelength of  $\sim 740$  nm is a compromise at which the output energy of the pumping laser is high enough and the absorption of  $F_2^{+ \cdot \cdot}$  centers is still sufficient for effective lasing.

In present work, we used a flash-lamp pumped alexandrite laser PAL-101 (Light Age, Inc.), operated at 20 Hz with energy per pulse up to 250 mJ at 740 nm and pulse width  $\sim 50$  ns. The output beam, with diameter  $\sim 3$  mm, had smooth multimode spatial structure and divergence of  $< 1$  mrad.

The lasing spectrum for the  $LiF:F_2^{+ \cdot \cdot}$  laser with a non-selective resonator under alexandrite laser pumping (740 nm) is shown in Fig. 1 (curve 3) with a maximum at 950 nm and bandwidth of 30–40 nm (FWHM). The input-output curve for this laser with a 50% output coupler is shown in Fig. 2 (curve 1) with the slope efficiency of  $\sim 31\%$ . The lasing threshold was estimated to be  $\sim 150$  mJ/cm<sup>2</sup>. A maximum output average power of 1.4 W was achieved with 5 W of input power at 740 nm incident onto the crystal (real efficiency  $\sim 28\%$ ). It is necessary to point out that some laser properties of  $F_2^{+ \cdot \cdot}$ -like centers under alexandrite laser pumping were briefly discussed by Lobanov and Kostyukov [11].

In order to measure the tuning range, the output coupler was replaced with a plane diffraction grating (1200 grooves/mm) in Littrow configuration. The efficiency of diffraction in the first order was  $\sim 30\%$ . The experimental tuning curve extended from 820 to 1120 nm and is shown in Fig. 3 (1). By replacing the input dichroic mirror (optimal for 875–1040 nm range) with a mirror which had high reflectivity at 780–920 nm (low reflectivity at 950–1200 nm) the tuning range was extended towards shorter wavelengths up to 796 nm (Fig. 3 (2)), and with a mirror optimal for the long wavelength range (high reflectivity at 1000–1250 nm and low reflectivity at 800–1000 nm) the

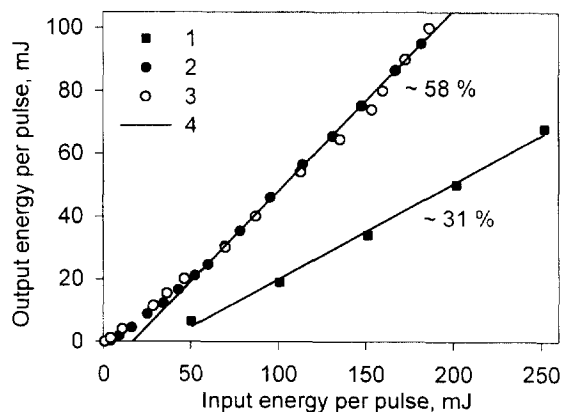


Fig. 2. Input/output dependences for  $LiF:F_2^{+ \cdot \cdot}$  laser at 300 K with non-selective resonator under pumping with: (1)  $\lambda_{pump} = 740$  nm, and (2)  $\lambda_{pump} = 683$  nm, (3)  $\lambda_{pump} = 633$  nm. Line (4) is a linear fit.

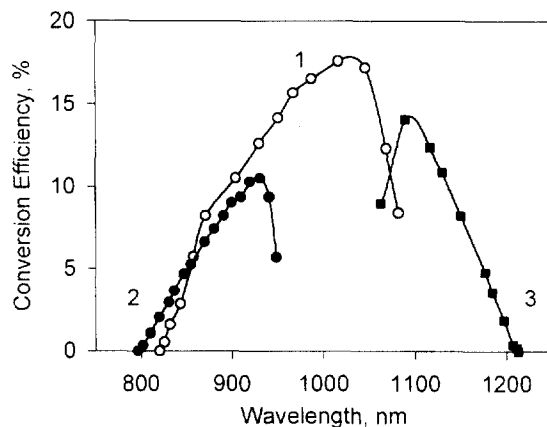


Fig. 3. Tuning curve for  $LiF:F_2^{+ \cdot \cdot}$  laser at 300 K ( $\lambda_{pump} = 740$  nm, pulse energy incident on the crystal  $\sim 145$  mJ,  $t_{pulse} \sim 50$  ns).

tuning range was extended up to 1210 nm (Fig. 3 (3)). The obtained tuning range is much wider than previously reported [3–5]. The width of  $LiF:F_2^{+ \cdot \cdot}$  laser pulses, both with a dispersive and with a non-selective resonator, was very similar and equal to  $\sim 40$  ns.

We also investigated operation of a  $LiF:F_2^{+ \cdot \cdot}$  laser under 683 nm and 633 nm pumping. Laser radiation at these wavelengths with energy per pulse up to 250 mJ, pulse width  $\sim 6$  ns, repetition rate 10 Hz, and low divergence  $< 0.5$  mrad was obtained by Raman shifting the second harmonic of a pulsed Nd:YAG laser (GCR-230, Spectra Physics, Inc.) in hydrogen (683 nm) or deuterium (633 nm).

The same non-selective resonator (as with alexandrite laser pumping) was used but the output coupler had 10% reflectivity. A much higher slope efficiency of 58% and real conversion efficiency of  $\sim 53\%$  were obtained with 683 and 633 nm pumping (see Fig. 2, curves 2 and 3). The efficiency was higher than for alexandrite laser pumping because: (i) the 633 and 683 nm wavelengths are closer to the absorption peak (620 nm) of  $F_2^{+ \cdot \cdot}$  centers (the ratio of absorption of the coefficients  $k$  is  $k_{633 \text{ nm}}/k_{740 \text{ nm}} = 4.8$ ,  $k_{683 \text{ nm}}/k_{740 \text{ nm}} = 2.9$ ), and (ii) the temporal relationship between the laser pulse width and luminescence decay time ( $\tau_{lum} = 20$  ns at 300 K) is different:  $t_{pulse} = 6$  ns  $< \tau_{lum}$  for the 633 and 683 nm pumping, and  $t_{pulse} = 50$  ns  $> \tau_{lum}$  for the alexandrite laser. The lasing threshold of 6–8 mJ/cm<sup>2</sup> under 633 and 683 nm pumping was also lower (even with 10% reflectivity of output coupler). Although the absorption of  $F_2^{+ \cdot \cdot}$  centers at 633 nm is 1.7 times higher than at 683 nm there is only a slight difference in the operation of the  $LiF:F_2^{+ \cdot \cdot}$  laser (see Fig. 2 curves 2 and 3). It can be explained by the fact that the characteristic absorption length ( $1/k$ ) at the pumping wavelength, although different at 633 nm (0.45 cm) and

683 nm (0.75 cm), is much less than the total length of the crystal (4 cm).

The width of LiF:F<sub>2</sub><sup>+</sup> laser pulses ( $\leq 6$  ns) was very close to the pulse width of the pumping laser radiation ( $\sim 6$  ns) at 633 or 683 nm. Low divergence and smooth profile of the pumping laser beam resulted in excellent spatial properties of LiF:F<sub>2</sub><sup>+</sup> laser output: smooth multi-mode beam profile with divergence  $< 2$  mrad.

In our experiments, LiF:F<sub>2</sub><sup>+</sup> crystals did not exhibit any photodegradation when pumped by radiation in the 620–750 nm range at energy densities of up to  $\sim 5$  J/cm<sup>2</sup>. We estimated the lifetime of these color center crystals to exceed 10 years at room temperature. The maximum output power of the LiF:F<sub>2</sub><sup>+</sup> laser was limited by the capabilities of the available pumping lasers.

The tuning range of the LiF:F<sub>2</sub><sup>+</sup> laser partially overlaps with the emission band of commonly used Ti:sapphire lasers. The luminescence bandwidth is similar for both materials (185 nm for LiF:F<sub>2</sub><sup>+</sup> and 175 nm for Ti:sapphire) but the luminescence peak for F<sub>2</sub><sup>+</sup> centers is shifted toward longer wavelengths (890 nm – F<sub>2</sub><sup>+</sup>, 760 nm – Ti). The main difference lies in the value of emission lifetime and cross-section. Ti:sapphire has relatively low emission cross-section ( $2.7 \times 10^{-19}$  cm<sup>2</sup>) as compared with the LiF:F<sub>2</sub><sup>+</sup> crystal ( $5.7 \times 10^{-17}$  cm<sup>2</sup>). The consequences of that for Ti:sapphire are a high lasing threshold ( $\sim 1$  J/cm<sup>2</sup>), about 400 times higher than for LiF:F<sub>2</sub><sup>+</sup> ( $2.5 \times 10^{-3}$  J/cm<sup>2</sup>) and a lack of temporal overlapping of pump and generated pulses. (These values of lasing threshold were estimated for a resonator with 100% reflective mirrors.) Poor temporal overlapping makes it very difficult to perform nonlinear frequency mixing of pump and generated laser beams with pulsed Ti:sapphire lasers. Contrary, LiF:F<sub>2</sub><sup>+</sup> laser is free of this shortcoming.

A LiF:F<sub>2</sub><sup>+</sup> laser combines the advantages of a dye laser, such as high quantum efficiency, large emission cross section, and wide tuning range, with the advantages of solid state laser media. The other very important feature, almost unreachable for dye lasers and OPOs, is the possibility for easy scaling of a LiF:F<sub>2</sub><sup>+</sup> laser. Crystal sizes as large as  $\varnothing 400 \times 200$  mm can be achieved for LiF.

#### 4. Conclusion

In conclusion, simultaneous solution of the problems related to thermal degradation and optical bleaching of F<sub>2</sub><sup>+</sup>-like color centers in LiF crystals allowed us to develop a highly efficient room-temperature-stable color center laser with significantly enhanced 820–1210 nm tuning range. A LiF:F<sub>2</sub><sup>+</sup> laser with record output power (up to  $\sim 1.4$  W) and energy ( $\sim 100$  mJ) parameters and real efficiency of about 28% under alexandrite laser pumping and 53% under 683 nm or 633 nm pumping has been demonstrated.

#### Acknowledgements

This work was partially supported by NSF/EPSCoR grant OSR-9550480.

#### References

- [1] L.F. Mollenauer, in: L.F. Mollenauer, J.C. White (Eds.), *Tunable Lasers*, Vol. 59, Springer, Berlin, 1987, pp. 225–277.
- [2] T.T. Basiev, S.B. Mirov, *Room Temperature Tunable Color Center Lasers*, Vol. 16, Harwood Acad. Publ., Chur, Switzerland, 1994, pp. 1–160.
- [3] V.M. Khulugurov, B.D. Lobanov, *Sov. Tech. Phys. Lett.* 4 (1978) 595.
- [4] T.T. Basiev, V.A. Konyushkin, S.B. Mirov, V.V. Ter-Mikirtychev, *Sov. J. Quantum Electron.* 22 (1992) 128.
- [5] V.V. Ter-Mikirtychev, *Appl. Optics* 34 (1995) 6114.
- [6] J. Nahum, *Phys. Rev.* 158 (1967) 814.
- [7] S.B. Mirov, A.Yu. Dergachev, *Proc. SPIE* 2986 (1997) 162.
- [8] Ch. Lushchik, I.K. Vitol, M.A. Elango, *Sov. J. Solid State Physics* 10 (1968) 2753.
- [9] Ch.B. Lushchik, I.K. Vitol, M.A. Elango, *Usp. Fiz. Nauk.* 122 (1977) 223.
- [10] I.A. Parfianovich, V.M. Khulugurov, B.D. Lobanov, N.T. Maksimova, *Bull. Acad. Sci. USSR Phys. Ser.* 43 (1979) 20.
- [11] B.D. Lobanov, V.M. Kostyukov, *Proc. SPIE* 1839 (1991) 265.